A 3D Correlation Model for MIMO Non-Isotropic Scattering with Arbitrary Antenna Arrays

Hamidreza Saligheh Rad and Saeed Gazor
Department of Electrical and Computer Engineering
Queen's University, Kingston, Ontario, K7L 3N6, Canada
Tel: (613) 533-6068, Fax: (613) 533-6615
radh,gazors@ee.queensu.ca

Abstract— **In this paper we introduce a Multiple-Input Multiple-Output (MIMO) space-time-frequency wireless channel model for the wave propagation in the three-dimensional (3D) space. The Cross-Correlation Function (CCF) between two sub-channels of the MIMO communication system is decomposed into some non-negative functions. These functions are expressed in terms of a selection of channel parameters such as the carrier frequencies, the delay profile, the pathloss exponent, the softness factor θ, the non-uniform distribution of direction of arrivals and departures, array geometries, and the mobile speed. We introduce a class of distributions for the Elevation Angle (EA) spreads as a basis such that any arbitrary (isotropic or non-isotropic) EA distribution can be represented by a convex linear combination of this class. The corresponding term of the CCF of the 3D-MIMO model for any EA distribution equals to the same linear combination of the basis CCF terms associated to the class. This 3D-MIMO model formulates the CCF as a function the spacial separation of antennas, time, and carrier frequencies in terms of physical channel parameters such as mobile speed, delay profile and distribution of scavengers around mobile and base station.**

Keywords: **Wireless channel modeling, Cross-Correlation Function, 3D Non-Isotropic Wave Propagation.**

I. Introduction

Space-Time (ST) channel models are required to evaluate the performance of a Multiple-Input Multiple-Output (MIMO) communications system in the presence of fading(s). Existing MIMO channel models are usually either idealistically simple or too complicated for such an analysis. Moreover, most of existing MIMO models assume wave propagation in a two-dimensional (2D) space, and consider a special geometry (usually one-ring [2], [3]) for the local scatterers, combined with appropriate probability density functions (PDFs) for the physical parameters.

In this paper, we introduce a 3D-MIMO model by considering a series expansion for any spatial distribution of scatterers around the Mobile Station (MS) and the Base Station (BS), allowing characterization of various environments, e.g., macro-microcellular, isotropic or non-isotropic, flat-fading or frequency-selective, spherical or cylindrical scattering distribution. We specifically calculate the Cross-Correlation Function (CCF) of two sub-channels between two pairs of antenna elements in the MS and the BS [4], [6], assuming any given. We use the Fourier series expansion of the PDF of the non-isotropic azimuth of arrivals and departures and a general EA distribution in the third dimension in order to characterizers various 3D non-isotropic environments. This model can be used in the design and the performance evaluation of wireless communication systems.

Several researchers have recently proposed for 3D channel models for Single-Input Single Output (SISO) and MIMO communication systems, e.g., [8]–[16]. Aulin introduced a 3D-SISO channel model [8]. He assumed that the spatial angle of arrival in the horizontal plane is uniformly distributed in all directions, and is non-uniformly distributed for vertical angle of arrival. This model fits better to the empirical results compared with the two-dimensional (2D) model proposed in [20]. Turkmani and Parsons [9], [10] suggested a more realistic scatterer distribution for vertical angle of arrival. They derived an expression for the spatial CCF between antenna elements in the BS, and evaluated the impact of various physical parameters. Falconer and Roy [11] proposed a wideband 3D-model based on [9], [10] considering the beam-pattern of BS antenna elements. Qu and Yeap [12] suggested a family of PDFs with two parameters, for symmetrical and asymmetrical distributions of the elevation angle (EA). Some of these PDFs lead to analytical expressions for the Power Spectral Density (PSD) of the channel. A combination of these PDFs allow modeling of a wide range of environments. Fitz and Mohasseb [13] proposed a 3D generalization of the Jake's model [20] for a MIMO system based on a geometrical distribution of scatterers and ideas from [8]–[10]. Theses models consider many relevant physical parameters; however, they mostly assume a specific geometry of scatterers in the environment. Moreover, the integral expression of the CCF for these methods needs to be numerically evaluated. Abhayapala, Pollock, and Kennedy [14] developed a 3D spatial channel model to provide insight into spatial aspects of MIMO systems. They used the spherical harmonic representation wavefields to decompose spatial channel matrix into a product of known and random matrices where the known portion shows the effects of the physical configuration of antenna elements. Yong and Thompson [15] derived an spatial fading correlation function for a Uniform Rectangular Array (URA) and a 3D multipath channel. This CCF is expressed in terms of azimuth and elevation angles of arrivals and the geometry of the array. Results demonstrate that azimuth spread (AS) is one of the primary determinant of the antenna correlation and the impact of the elevation spread is mainly noticeable at low AS values. Yao and Patzold [16] investigated the spatial-temporal characteristics of a 3D theoretical channel model for scatterers which form a half-

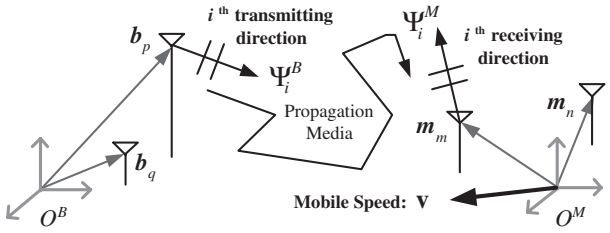

Fig. 1. p^{th} (q^{th}) antenna element of BS and m^{th} (n^{th}) antenna element of MS in their local coordinate axis in a 3D wave propagation environment. The i^{th} transmitting direction $\mathbf{\Psi}_i^B$ (i^{th} receiving direction $\mathbf{\Psi}_i^M$) from the i^{th} dominant propagating waveform between this antenna pair is also shown.

spheroid with a given axial length ratio. In this paper, we extend the 2D-MIMO model proposed by Gazor and Rad [4], [6] into a realistic 3D-MIMO model.

In Section II, the notations are defined and assumptions on the parameters of the propagation media are described. The proposed 3D ST CCF is calculated in Section III, in the presence of Doppler fading and environment correlation. We use family of PDFs such that any PDF for the EA can be expressed by a linear convex combination this family of distributions, and derive the CCF as the same linear combination of CCFs associated to these PDFs, allowing accurate modeling for various wireless propagation environments. The discussions and conclusions are made in Section IV.

II. Three-Dimensional MIMO Model Description

A pair of BS-MS antenna elements from a multielement antenna communication system in a 3D wave propagation environment is shown in Figure 1. Throughout this paper the following notations are used where the superscripts B and M indicate variables at the BS and the MS sides respectively:

O^B, O^M	BS coordinate, MS coordinate;
ω	Carrier frequency;
$h_{mp}(t,\omega)$	Channel Impulse Response (CIR) between p^{th} BS antenna and m^{th} MS antenna;
$\mathbf{b}_p$	Position vector of the p^{th} antenna element on the BS side relative to O^B;
$\mathbf{m}_m$	Position vector of the m^{th} antenna element on the MS side relative to O^M;
$\mathbf{v}$, c	MS speed vector, Wave propagation velocity;
$\mathbf{\Psi}_i^B$	Unity vector pointing to the Direction of Departure (DOD) of the i^{th} waveform from the BS;
$\mathbf{\Psi}_i^M$	Unity vector pointing to the Direction of Arrival (DOA) of the i^{th} waveform to the MS;
Θ_i^B	The i^{th} DOD azimuthal angle from the BS;
Θ_i^M	The i^{th} DOA azimuthal angle to the MS;
Ω_i^B	The i^{th} DOD elevation angle from the BS;
Ω_i^M	The i^{th} DOA elevation angle to the MS;
$\tau_{p,m;i}$	Delay between p^{th} BS antenna element and m^{th} MS antenna element via i^{th} dominant path;
$g_{p,m;i}$	Gain between p^{th} BS antenna element and m^{th} MS antenna element via the i^{th} dominant path, approximated by g_i;
ϖ_i	The shifted frequency for the i^{th} dominant path, caused by the Doppler effect;
ϕ_i	Phase contribution along the i^{th} dominant path;
θ, η	Softness factor, Pathloss exponent;
$\overline{\tau}$, σ^2	Mean and Variance of the time-delay τ_i; and,
α, I	Degree of Urbanization, Number of total waves.

Note $\Psi_i \triangleq [\cos(\Omega_i)\cos(\Theta_i), \cos(\Omega_i)\sin(\Theta_i), \sin(\Omega_i)]^T$ [24]. Consider a moving MS with the constant speed $\mathbf{v}(\frac{\text{m}}{\text{sec}})$ and a fixed BS in Figure 1. Antenna elements are arbitrarily located in the 3D space at the MS and BS sides around their local coordinates, O^B and O^M. We assume that the antennas are omnidirectional and are addressed by position vectors with respect to their local coordinates, e.g., $\mathbf{b}_p$ and $\mathbf{m}_m$. We also assume that propagated waves are planar. This assumption is justified provided that the distance between scatterers and antenna arrays is much larger compared to the inter-element antenna distances [1, Page 75]. Such assumption implies that there is no inter-element scattering, i.e., DODs and DOAs do not depend on the antenna indices. Each array antenna element $\mathbf{m}_m$ receives the signal through the media via a large number of dominant propagating paths with different lengths. The Line-Of-Sight (LOS) propagation path between the transmitter and the receiver can be deterministically treated [3]. We assume no LOS. In addition, we assume identical PDFs for physical parameters in all directions in space.

By breaking down the received waveform into a linear combination of plane waves, we can achieve a solution based on Maxwell's equations [1], [23]. Each component in this equation is the direct result of scattering effect in the propagation environment; each received waveform is associated with a path attenuation gain $g_{p,m;i}$ and a path phase shift ϕ_i. The path gain represents pathloss and the fading effects of the propagation waves along the path. The path phase change represents the contribution of the path on the phase of the received signal. CIR of such a process is represented as a function of the carrier frequency as,

$$h_{mp}(t,\omega) \triangleq \sum_{i=1}^{I} g_{p,m;i} \exp\left(j\phi_i - j\omega\tau_{p,m;i}(t)\right), \qquad (1)$$

where I is the number of dominant paths resulting from scattering, $\tau_{p,m;i}(t)$ is the time-delay over i^{th} path and $g_{p,m;i}$ is the real gain of the i^{th} dominant path between $\mathbf{b}_p$ and $\mathbf{m}_m$. The gain, $g_{p,m;i}$, is a function of the time-delay and the slow fading factor [3], [19]. The propagation delay over i^{th} path, $\tau_{p,m;i}(t) \triangleq \tau_{p,m;i} + \frac{t}{c}\mathbf{v}^T\mathbf{\Psi}_i^M$, is time-varying due to the mobility of MS. Substituting the time-varying delay in (1), CIR of such a propagation environment is represented by,

$$h_{mp}(t,\omega) = \sum_{i=1}^{I} g_{p,m;i} \exp\left(j\phi_i - j\varpi_i t - j\omega\tau_{p,m;i}\right), \qquad (2)$$

where the shifted frequency of the i^{th} received waveform caused by the Doppler effect is denoted by Doppler shift $\varpi_i \triangleq \frac{\omega}{c}\mathbf{v}^T\mathbf{\Psi}_i^M$, ω is the carrier frequency, and $\mathbf{v}$ and c are the MS velocity vector and the speed of light, respectively. Notation ϕ_i is the phase change of the signal along the i^{th} path. Time dependency of $h_{mp}(t,\omega)$ is mainly due to the effect of user mobility, i.e., the Doppler effect [1]. The term $\frac{1}{\sqrt{I}}$ is introduced to retain a constant energy random process, i.e.,

to guarantee the convergence of $I^{-1}\sum_{i=1}^{I} E[g_i^2]$ as $I \to \infty$. In this paper we make some statistical assumptions on the physical parameters of 3D propagation environment [4], [6].

A1) We decompose the i^{th} path propagation delay, $\tau_{p,m;i}$, into three components: one major distance delay, and two relative propagation delays with respect to local coordinates across the BS and MS antenna arrays. This delay can be written in the following form

$$\tau_{p,m;i} = \tau_i - (\tau_{p;i}^B + \tau_{m;i}^M), \tag{3a}$$

$$\tau_{p;i}^B \triangleq \frac{\mathbf{b}_p^T \mathbf{\Psi}_i^B}{c}, \tag{3b}$$

$$\tau_{m;i}^M \triangleq \frac{\mathbf{m}_m^T \mathbf{\Psi}_i^M}{c}, \tag{3c}$$

where τ_i represents distance delay between O^B and O^M, and $\tau_{p;i}^B$ and $\tau_{m;i}^M$ represent relative propagation delays from antenna elements, $\mathbf{b}_p$ or $\mathbf{m}_m$, to corresponding coordinates [19]. We consider independent identically distributed (i.i.d.) Exponential pdf for the distance delay τ_i as a common delay distribution for outdoor environments [2]. This distribution is defined as $\tau_i \sim \frac{1}{\sigma} e^{-\frac{x-\overline{\tau}+\sigma}{\sigma}}$, $\forall x \geqslant \overline{\tau}-\sigma$, where $\overline{\tau}$ is the mean value to specify the distance between the MS and BS (major propagation distance), and σ^2 is the variance of this distribution. The moment-generating-function (MGF) of the time-delay pdf is given by:

$$\mathbf{\Phi}_\tau(s) = \frac{e^{(\overline{\tau}-\sigma)s}}{1-\sigma s}. \tag{4}$$

A2) Path gain, $g_{p,m;i}$, and propagation delay, $\tau_{p,m;i}$, are random parameters and are functions of path length. The relationship between $g_{p,m;i}$ and the average pathloss power, $P(\tau_{p,m;i})$, is justified by experimental measurements to be $g_{p,m;i} \triangleq \sqrt{\frac{P(\tau_{p,m;i})}{I}}$ [19], [21]. The shadowing effect or slow fading is not considered in this paper. By experimental measurements it is found that the dependency of the pathloss on the time-delay, $\tau_{p,m;i}$, is characterized by [22, Page 38]

$$P(\tau_{p,m;i}) \triangleq P_0 \left(\tau_{p,m;i}\right)^{-\eta}, \tag{5}$$

where η is called pathloss exponent, and P_0 is a constant. Depending on the propagation media, the pathloss exponent is measured between 2 and 6 [22], [23]. From (5), (3a) and the obvious fact that $|\tau_i| \gg \max\left\{|\tau_{p;i}^B|, |\tau_{m;i}^M|\right\}$, we approximate $P(\tau_{p,m;i}) \simeq P(\tau_i)$ for all the BS and MS antennas as:

$$g_{p,m;i} \simeq g_i = \sqrt{\frac{P_0}{I}} \left(\tau_i\right)^{-\frac{\eta}{2}}. \tag{6}$$

A3) We consider the phase contribution of surrounding scatterers by a random phase change, $\phi_i \sim U[-\pi, \pi)$. It makes sense to impose some restriction to the phase differences of similar paths $\delta = \phi_{i_1} - \phi_{i_2}$ [4]. These phase changes are assumed to be independent. For two similar paths i_1 and i_2, we assume a pdf for $\delta = \phi_{i_1} - \phi_{i_2}$ as: $p_{\boldsymbol{\delta}}(\delta) \sim U[-\theta, \theta) \otimes U[-\theta, \theta)$, where $\otimes$ stands for the circular convolution. The softness factor, $\theta \in [0, \pi)$, characterizes the effect of the environment on the phase change correlation. The number of such similar paths for a given path is limited by $I_{\text{sim}} < I$.

A4) The general form for the azimuth angular distribution; Θ_i^B and Θ_i^M, are defined over $[0, 2\pi)$. The pdf of such a distribution is represented by $f_{\mathbf{\Theta}_i}(\Theta_i)$, where $\Theta_i \triangleq \angle \mathbf{\Theta}_i$ [7]. This general distribution is expanded based on the fourier series expansion of periodic signals with period 2π, $f_{\mathbf{\Theta}_i}(\Theta_i) = f_{\mathbf{\Theta}_i}(\Theta_i + 2\pi)$ [24]:

$$f_{\mathbf{\Theta}_i}(\Theta_i) = \sum_{l=-\infty}^{+\infty} A_l \; e^{jl\Theta_i}, \tag{7a}$$

where,

$$A_l \triangleq \frac{1}{2\pi} \int_{-\pi}^{\pi} f_{\mathbf{\Theta}_i}(\Theta_i) e^{-jl\Theta_i} d\Theta_i. \tag{7b}$$

Without loss of generality, we assume a real-positive and even function for the angular distribution. It implies that the coefficients A_l are real and even; i.e., $A_l = A_l^*$ and $A_l = A_{-l}$ [24]. Using these properties, we will calculate and simplify the CCF in the next section. Exact empirical verifications are necessary in order to choose the appropriate shape of the azimuth PDF for the specified propagation scenario. Based on some valid measurement results and the fourier series analysis, in [7] we present a complete investigation on the Normal and Laplace azimuth distributions with a limited number of sinusoidal components. In addition, we assume that azimuth DODs and DOAs are independent from each other and from time-delays, $\tau_{p,m;i}$ [2], [3].

A5) The Elevation Angles are all independent and identically distributed $p_{\mathbf{\Omega}}(\Omega)$. It is clear that the majority of incoming/outgoing waves do travel in nearly horizontal directions. The determination of the EA distribution of such waves requires some considerations as it depends on the environment parameters like the degree of urbanization [9]. This determination has attracted the attention of some theoretical/experimental researchers [8], [9], [12], [17], [18]. Aulin in [8] and Parsons and Turkmani in [9] suggest realistic PDFs for EA in a microcellular scattering environment. These PDFs do not result in closed-form or easy to handle expressions for the CCF in the case of MIMO systems. Qu and Yeap [12] suggest a family of PDFs with two parameters for both the symmetrical and asymmetrical PDFs of the EA. Some of the PDFs lead to analytical solutions for the PSD of the received signal in a SISO system. Kuchar, Rossi and Bonek [17] measure the angular power distribution at the mobile station in downtown Paris at 890 MHz. According to this work, propagation over the roofs is significant; typically 65% of energy is incident with elevation larger than 10°. Authors of [18] measure the EA distribution at a mobile station in different radio propagation environments at 2.15GHz. Results show that in non-LOS situations, the power distribution in elevation has a shape of a double-sided exponential function, with different slopes on the negative and positive sides

of the peak. The slopes and the peak elevation angle depend on the environment and the BS antenna height. In order to satisfy the requirements for a PDF of realistic EAs previously proposed in the literature, we consider a simple family of distributions for $|\Omega| \leqslant \frac{\pi}{2}$ as [5]

$$\text{Case I:} \quad p_{\mathbf{\Omega}}(\Omega) = \frac{\Gamma(\alpha+1)\cos^{2\alpha}(\Omega)}{\sqrt{\pi}\,\Gamma(\alpha+\frac{1}{2})}, \quad (8a)$$

$$\text{Case II:} \quad p_{\mathbf{\Omega}}(\Omega) = \frac{2|\sin(\Omega)|^{2\alpha}\cos(\Omega)}{2\alpha+1}, \quad (8b)$$

where $\Gamma(z) = \int_0^\infty u^{z-1}e^{-u}du$ is the Gamma function [24, Page 258], and $\alpha \geqslant 0$ is related to the degree of urbanization. The parameter α specifies the type of the environment in the sense that the amount of waves scattered into the third dimension of the space. Selected distributions is a general class of functions suggested in [5]. Interestingly, a linear convex combination of the members of this class as a PDF covers a wide class of distributions and can realistically model a non-isotropic environment. Therefore, a linear convex combination of obtained results characterizes a wide class of non-isotropic propagation in the elevation. Experimental data can be used to interpolate for the calculation of the coefficients of this linear combination.

III. Three-Dimensional Space-Time Cross-Correlation Function

Based on established assumptions in the previous section, we derive a closed-form expression for the ST-CCF between the CIRs of two arbitrary communication links, $h_{mp}(t_1,\omega_1)$ and $h_{nq}(t_2,\omega_2)$. This CCF is denoted by [4]

$$R_{mp,nq}(t_1,t_2;\omega_1,\omega_2) \triangleq E[h_{mp}(t_1,\omega_1)\; h^*_{nq}(t_2,\omega_2)], \quad (9)$$

and is a function of sampling times (t_1,t_2), carrier frequencies (ω_1,ω_2) and antenna elements $(m,p;n,q)$.

By replacing (2) and (3) in (9), the ST-CCF between two sub-channels, CCF is written as follows

$$R_{mp,nq}(t_1,t_2;\omega_1,\omega_2) = E\Big[\sum_{i_1,i_2=1}^{I} g(p,m;i_1)g(q,n;i_2)\times e^{j(\omega_1\tau_{i_1}-\omega_1\tau_{i_1}+\phi_{i_1}-\phi_{i_2})}F_{i_1}F^*_{i_2}\Big], \quad (10a)$$

where,

$$F_{i_1} \triangleq e^{j(\varpi_{i_1}t_1+\frac{\omega_1}{c}\{\mathbf{b}_p^T\mathbf{\Psi}^B_{i_1}+\mathbf{m}_m^T\mathbf{\Psi}^M_{i_1}\})}, \quad (10b)$$

$$F_{i_2} \triangleq e^{j(\varpi_{i_2}t_2+\frac{\omega_2}{c}\{\mathbf{b}_q^T\mathbf{\Psi}^B_{i_2}+\mathbf{m}_n^T\mathbf{\Psi}^M_{i_2}\})}, \quad (10c)$$

and $\varpi_{i_1} \triangleq \frac{\omega_1}{c}\mathbf{v}^T\mathbf{\Psi}^M_{i_1}$ and $\varpi_{i_2} \triangleq \frac{\omega_2}{c}\mathbf{v}^T\mathbf{\Psi}^M_{i_2}$ are shifted frequencies [4], [6].

By regrouping dependent and independent random variables in (10a), replacing g_i from (6), and using Assumptions A1-4, the expression of the CCF in (10), $R_{mp,nq}(t_1,t_2;\omega_1,\omega_2)$, is decomposed as follows

$$R_{mp,nq}(t_1,t_2;\omega_1,\omega_2) = \frac{P_0}{I}\sum_{i_1,i_2=1}^{I}\Big\{E\Big[(\tau_{i_1}\tau_{i_2})^{\frac{-\eta}{2}}\,e^{j\left(\omega_2\tau_{i_2}-\omega_1\tau_{i_1}\right)}\Big] \times E\left[\exp(j(\phi_{i_1}-\phi_{i_2}))\right]E\left[F_{i_1}F^*_{i_2}\right]\Big\}. \quad (11)$$

In [4, Appendix I], each term in the above double-sum is calculated for a 2D wave propagation scenario. Similarly, after calculating the parts that do not depend on the angular distributions, we obtain

$$R_{mp,nq}(t_1,t_2;\omega_1,\omega_2) = \quad (12a)$$
$$= P_0\Pi^B_{p,q}\Pi^M_{m,n}\mathbf{\Phi}^{(\eta)}_\tau(j(\omega_2-\omega_1)) + $$
$$+\frac{P_0\sin^2\theta}{\theta^2}\Pi^B_p\Pi^B_q\Pi^M_m\Pi^M_n I_{\text{sim}}\mathbf{\Phi}^{(\frac{\eta}{2})}_\tau(-j\omega_1)\mathbf{\Phi}^{(\frac{\eta}{2})}_\tau(j\omega_2),$$

where $\mathbf{\Phi}^{(\eta)}_\tau(s)$ is obtained by η^{th}-times integrating the MGF, $\mathbf{\Phi}_\tau(s)$ [24]. In Assumption A1, we consider Exponential distribution for the delay profile. The expressions of $\mathbf{\Phi}^{(\eta)}_\tau$ are given in [4] by performing these integration on $\mathbf{\Phi}_\tau(s)$. The values $\Pi^{(.)}_{(.)}$ are calculated in terms of the following 3D vectors,

$$\mathbf{d}^B_{p,q} \triangleq \omega_1\mathbf{b}_p - \omega_2\mathbf{b}_q\ , \quad (12b)$$
$$\mathbf{d}^M_{m,n} \triangleq (\omega_1 t_1-\omega_2 t_2)\,\mathbf{v} + (\omega_1\mathbf{m}_m-\omega_2\mathbf{m}_n)\ ,$$
$$\mathbf{d}^B_p \triangleq \omega_1\mathbf{b}_p\ ,\quad \mathbf{d}^B_q \triangleq \omega_2\mathbf{b}_q\ , \quad (12c)$$
$$\mathbf{d}^M_m \triangleq \omega_1 t_1\mathbf{v}+\mathbf{m}_m\ ,\quad \mathbf{d}^M_n \triangleq \omega_2 t_2\mathbf{v}+\mathbf{m}_n\ ,$$

by employing the above superscripts, B or M and subscripts indices for $\mathbf{d}^{(.)}_{(.)} = [d_x,\ d_y,\ d_z]^T$, in the following functions,

$$\Pi \triangleq E_\Omega\left[e^{\Lambda_1\sin(\Omega)}\Upsilon\left(\Lambda_2\cos(\Omega)\right)\right], \quad (12d)$$

$$\Upsilon(z) \triangleq J_0(z)+4\pi\sum_{l=1}^{\infty}A_l j^l J_l(z)\cos l(\arctan\frac{d_y}{d_x}),$$

$$\Lambda_1 \triangleq \frac{d_z}{c} \quad\text{and}\quad \Lambda_2 \triangleq \frac{\sqrt{(d_x)^2+(d_y)^2}}{c}, \quad (12e)$$

where $J_l(z) \triangleq \frac{j^{-l}}{\pi}\int_0^\pi e^{jz\cos u}\cos(lu)du$ is the l^{th}-order Bessel function of the first kind [24, Page 360], $|.|$ denotes the Euclidian norm, and A_l is defined in the Assumption A4, $E_\Omega[.]$ is the expectation of $[.]$ using the PDF of Ω. Parameters $d^B_{(.)}$ and $d^M_{(.)}$ represent shifted distances at the BS and MS respectively [4], [6].

Remark 1: This model proposes the CCF between any two sub-channels of a 3D-MIMO wireless propagation environment when DODs and DOAs are non-uniformly distributed in both azimuth and elevation. In other words, the above CCP represents one of the elements of the channel correlation matrix.

Remark 2: The proposed 3D model takes into account the antenna heights [13]. The vertical separation of antenna elements is the result of their different heights. Such a difference in the antenna heights produces phase differences between the received or transmitted signals and consequently impact on the CCF. This property can be employed to improve the space diversity in wireless systems [23].

Remark 3: The CCF in the form of (12) appears in a linear convex series expansion form of Bessel functions of the first kind. This coefficients of this expansion are obtained by the fourier series expansion of the PDF of the azimuth angular spread. In practice for any common non-uniform azimuth distribution such as Normal and Laplace distributions, the underlined expansion is very well approximated by a limited number of its most important components. Thus, a summation only most important components should be enough to accurately represent any practical non-isotropic environment.

In general, the terms $\Pi^{(.)}_{(.)}$ have not closed-form expression. In Appendix I, we propose a computation method for the expectation integral Π. This solution is based on an expansion series of Bessel functions of the first kind. If there is no closed-form expression for CCF, this method can be numerically approximated. Following, we find closed-form solutions under some particular simplified conditions. These expressions give insight and physical interpretations for the derived equations.

Case I, $\alpha = 0$, $d_z = 0$

This case represents a uniform 3D rich scattering environment. Using the following Bessel integration [24, Page 485]:

$$\int_0^{\frac{\pi}{2}} J_{2n}\left(2zsin(\xi)\right) d\xi = \frac{\pi}{2} J_n^2(z) \ ,$$

in (12), we get

$$\Pi = \sum_{l=0}^{\infty} J_{2l}^2 \left(\frac{d}{2c}\right). \tag{13}$$

This result is similar to the 2D scenario [4]; however, the 3D case introduces powers of the Bessel function [14]. This model is a direct 3D extension of the Jake's/Clark model [20].

In the following two cases closed-form CCFs are introduced for the isotropic scattering in azimuth when DODs and DOAs are uniformly distributed over $[0, 2\pi)$.

Case II, $\alpha = \frac{1}{2}$, $d_z = 0$

In this case scatterers are uniformly distributed on a sphere. Using the following Bessel integration expression [24, Page 485]:

$$\int_0^{\frac{\pi}{2}} J_\zeta\left(z\sin(\xi)\right) \sin^{\zeta+1}(\xi) \cos^{2\nu+1}(\xi) d\xi =$$
$$= \frac{2^\nu \Gamma(\nu+1)}{z^{\nu+1}} J_{\zeta+\nu+1}(z), \quad \mathrm{Re}(\zeta) > -1, \mathrm{Re}(\nu) > -1,$$

we obtain

$$\Pi = \sqrt{\frac{\pi}{2\Lambda_2}}\ J_{\frac{1}{2}}\left(\Lambda_2\right). \tag{14}$$

Using $J_{\frac{1}{2}}(z) = \sqrt{\frac{2}{\pi}} \frac{\sin(z)}{\sqrt{z}}$ [24, Page 437], the expression in (14) results in

$$\Pi = \frac{\sin(\Lambda_2)}{\Lambda_2} \triangleq \mathrm{sinc}\left(\Lambda_2\right). \tag{15}$$

This result is consistent with the available literature on isotropic 3D-SISO propagation [14].

Case III, $d_x = d_y = 0$

This case studies the vertical separation of antenna elements in a microcellular propagation environment. All antenna elements are located on the z-axis. In this case, using the following Bessel integration [24, Page 360]:

$$J_\nu(z) = \frac{(\frac{1}{2}z)^\nu}{\sqrt{\pi}\ \Gamma(\nu+\frac{1}{2})} \int_0^\pi \cos\left(z\cos(\xi)\right) \sin^{2\nu}(\xi) d\xi \ ,$$

we obtain

$$\Pi = \frac{\Gamma(\alpha+1)}{(\frac{1}{2}\Lambda_1)^\alpha}\ J_\alpha\left(\Lambda_1\right), \tag{16}$$

where α represents the degree of urbanization. This case characterizes different propagation environments by the degree of urbanization α.

Case IV, $d_z = 0$

Using (8b) and the Bessel integration [24, Page 485], we get

$$\Pi = \frac{2^{\alpha+\frac{3}{2}}\Gamma(\alpha+\frac{1}{2})}{(2\alpha+1)(\Lambda_2)^{\alpha+\frac{1}{2}}}\ J_{\alpha+\frac{1}{2}}\left(\Lambda_2^B\right). \tag{17}$$

This simple expression is another extension for the Jake's model for isotropic scattering environment.

IV. Conclusions

In this paper, we presented a cross-correlation model for MIMO wireless systems in the 3D space with respect to space, time and frequency. The resulting CCF between any two sub-channels of the MIMO communication system is composed of a summation of two non-negative terms; each term is decomposed into a multiplication of some non-negative functions. Each function describes (and provides insight about) the impact of some of key parameters of the physical propagation environment and communication system; e.g., the carrier frequencies, the array geometries at MS and BS, the non-uniform angular spread on azimuth and elevation, the delay profile, the path-loss exponent, the softness factor and the mobile speed. This decomposition/separation is a very flexible model to fit various practical MIMO channels and can charachterize formulate different propagation scenarios such as flat-fading or frequency-selective environments, micro-macrocellular scenarios, spherical or cylindrical wave propagation, etc [5]. Two of these multiplicative correlation terms are obtained by (η)-order and $(\eta/2)$-order integral of the MGF of the delay profile at the carrier frequency offset and at two carrier frequencies, respectively, where η is the environment pathloss exponent. Two other functions, Π^B and Π^M, describe the spatial effects of the BS and the MS, respectively. In general, resulting integrals do not have closed-form solutions. We obtained closed-form expressions of the CCF for a family of EA distributions. Since the PDF of EA can be expressed accurately by a linear convex combination of members of this class, the resulting CCF is exactly expressed in by the same linear combination in the form of a Bessel series expansion. In Appendix I a method for calculation of two expectation terms of CCF is given. This method allows to calculate the CCF for a

microcellular scenario. These terms represent the impact of the third spatial dimension of the propagation environment on the behaviour of the channel response. In Section III, closed-form expressions are derived for important cases in a 3D environment. Results of this paper are easy-to-use and mathematically tractable for simulation purposes and analytical analysis. This model also gives a better understanding of the complicated 3D non-isotropic propagation media.

APPENDIX I
GENERAL SOLUTION FOR THE 3D NON-ISOTROPIC CCF

In this Appendix, we calculate the integral Π for any non-isotropic scattering environment. This solution is given based on a polynomial series expansion of Bessel functions of the first kind. Using the following ascending series formula [24, Page 360],

$$J_\nu(z) = (\frac{1}{2}z)^\nu \sum_{k=0}^{\infty} \frac{(-\frac{1}{4}z^2)^k}{k!\Gamma(\nu+k+1)}, \tag{18}$$

for a l^{th}-order Bessel function, we get

$$\Pi = 4\pi\Lambda_3 \sum_{l=0}^{\infty} (\frac{1}{2}\Lambda_2)^l A_l j^l \cos(l\psi) \sum_{k=0}^{\infty} \frac{\left(-\frac{1}{4}(\Lambda_2)^2\right)^k}{k!\Gamma(l+k+1)} \times \tag{19}$$
$$\times \int_\Omega \cos\left(\Lambda_1 \sin(\Omega)\right) \cos^{2k+2\alpha+l}(\Omega) d\Omega$$

where Λ_1 and Λ_2 are defined in (12c) in terms of $\mathbf{d}_{(.)}^{(.)} = [d_x,\ d_y,\ d_z]^T$, and $\Lambda_3 \triangleq \frac{\Gamma(\alpha+1)}{\sqrt{\pi}\ \Gamma(\alpha+\frac{1}{2})}$ is a constant number defined by the complete gamma function. We calculate integral term in (19), using the following Bessel integration expression [24, Page 360]:

$$J_\nu(z) = \frac{(\frac{1}{2}z)^\nu}{\sqrt{\pi}\ \Gamma(\nu+\frac{1}{2})} \int_{-\frac{\pi}{2}}^{\frac{\pi}{2}} \cos(z\sin\xi)\cos^{2\nu}\xi\ d\xi\ , \tag{20}$$

and obtain,

$$\Pi = 4\pi \frac{\Gamma(\alpha+1)}{\Gamma(\alpha+\frac{1}{2})\left(\frac{1}{2}\Lambda_1\right)^\alpha} J_{\frac{l}{2}+k+\alpha}(\Lambda_1) \times \tag{21}$$
$$\times \sum_{l=0}^{\infty}\sum_{k=0}^{\infty} \frac{\Lambda_2^l A_l j^l \cos(l\psi)\ \Gamma(\frac{l+1}{2}+k+\alpha)(-\Lambda_2^2)^k(\frac{1}{2})^{k+\frac{l}{2}}}{k!\Gamma(l+k+1)(\Lambda)^{k+\frac{l}{2}}},$$

Note that $A_0 = \frac{1}{4\pi}$ and $\psi = \arctan(\frac{d_y}{d_x})$.

REFERENCES

[1] G. Durgin, *Space-Time Wireless Channels*, NJ: Prentice Hall, 2003.

[2] M. Kalkan and R. H. Clarke, "Prediction of the Space-Frequency Correlation Function for Base Station Diversity Reception," *IEEE Transactions on Vehicular Technology,* vol. 46, no. 1, pp. 176-184, Feb. 1997.

[3] A. Abdi and M. Kaveh, "A Space-Time Correlation Model for Multielement Antenna Systems in Mobile Fading Channels," *IEEE Journal on Selected Areas in Communications,* vol. 20, no. 3, pp. 550-560, April 2002.

[4] S. Gazor, and H. S. Rad, "Delay-Frequency Characterization of MIMO Wireless Channels," under review, *IEEE Transactions on Wireless Communications,* April 2004.

[5] H. S. Rad, S. Gazor, K. Shahtalebi, "Spatial-Temporal-Frequency Decomposition for 3D MIMO Microcell Uncorrelated Wireless Channels," *Canadian Conference on Electrical and Computer Engineering 2004 (CCECE'04),* Niagara Falls, May 2004.

[6] H. S. Rad, and S. Gazor, "MIMO Space-Time Correlation Model for Microcellular Environments," *Fifth IEEE Workshop on Signal Processing Advances in Wireless Communications,* Lisboa, Portugal, July 11-14, 2004.

[7] H. S. Rad, and S. Gazor, "Non-Isotropic Wave Propagation in MIMO Wireless Environments," submitted to *IEEE International Conference on Communications, ICC'05,* August 2004.

[8] T. Aulin, "A Modified Model for the Fading Signal at a Mobile Radio Channel," *IEEE Transactions on Vehicular Technology,* vol. VT-28, no. 3, pp. 182-203, August 1979.

[9] J. D. Parson, and A. M. D. Turkmani, "Characterisation of Mobile Radio Signals: Model Description," *IEE Proceedings I, Communications, Speech and Vision,* vol. 138, no. 6, pp. 549-556, December 1991.

[10] ——, "Characterisation of Mobile Radio Signals: Base Station Crosscorrelation," *IEE Proceedings I, Communications, Speech and Vision,* vol. 138, pp. 557-565, December 1991.

[11] S. Roy, and D. D. Falconer, "A Three-Dimensional Wideband Propagation Model for the Study of Base Station Antenna Arrays with Application to LMCS," *VTC'98,* Ottawa, August 1998.

[12] S. Qu, T. Yeap, "A three-dimensional scattering model for fading channels in land mobile environment," *IEEE Transactions on Vehicular Technology,* no. 3, vol. 48, pp. 765-781, May 1999.

[13] Y. Z. Mohasseb, and M. P. Fitz, "A 3D Spatio-Temporal Simulation Model for Wireless Channels," *IEEE Journal on Selected Areas in Communications,* vol. 20, no. 6, August 2002.

[14] T. D. Abhayapala, T. S. Pollock, and R. A. Kennedy, "Characterization of 3D Spatial Wireless Channels," *VTC 2003-Fall,* vol. 1, pp. 123-127, 2003.

[15] S. K. Yong, J. S. Thompson, "A three-dimensional spatial fading correlation model for uniform rectangular arrays," *Antennas and Wireless Propagation Letters,* no. 12, vol. 2, pp. 182-185, 2003.

[16] Q. Yao, M. Patzold, "Spatial-Temporal Characteristics of a Half-Spheroid Model and its Corresponding Simulation Model," *VTC 2004-Spring,* Milan.

[17] A. Kuchar, J.-P. Rossi, and E. Bonek, "Directional macro-cell channel characterization from urban measurements," *IEEE Transactions on Antennas and Propagation,* no. 2, vol. 48, pp. 137-146, Feb. 2000.

[18] K. Kalliola, K. Sulonen, H. Laitinen, O. Kivekas, J. Krogerus, P. Vainikainen, "Angular power distribution and mean effective gain of mobile antenna in different propagation environments," *IEEE Transactions on Vehicular Technology,* no. 5, vol. 51, pp. 823-838, Sept. 2002.

[19] M. Stege, J. Jelitto, M. Bronzel and G. Fettweis, "A Multiple Input - Mutiple Output Channel Model for Simulation of Tx and Rx Diversity Wireless Systems," *52nd IEEE Conference on Vehicular Technology*, vol. 2, pp. 833-839, 2000.

[20] W. C. Jakes, Ed., *Microware Mobile Communications*, New York: Wiley, 1974.

[21] H. L. Bertoni, *Radio Propagation for Modern Wireless Systems*, Prentice Hall PTR, 1999.

[22] T. S. Rappaport, *Wireless Communications - Principles and Practice*, Prentice Hall PTR, 1996. pp. 311-335, March 1998.

[23] S. Saunders, *Antennas and Propagation for Wireless Communication Systems*, New York: Wiley, 1999.

[24] M. Abramowitz, and I. A. Stegun, *Handbook of Mathematical Functions with Formulas, Graphs, and Mathematical Table,* Dover Publications INC., NY, June 1974.